THE JOURNAL OF BIOLOGICAL CHEMISTRY VOL. 280, NO. 47, pp. 39353–39362, November 25, 2005


# Angiotensin-converting Enzyme 2 (ACE2), But Not ACE, Is Preferentially Localized to the Apical Surface of Polarized Kidney Cells*

Received for publication, August 12, 2005 Published, JBC Papers in Press, September 15, 2005, DOI 10.1074/jbc.M508914200

**Fiona J. Warner[‡§1], Rebecca A. Lew[§], A. Ian Smith[§], Daniel W. Lambert[‡], Nigel M. Hooper[‡], and Anthony J. Turner[‡2]**

*From the [‡]Proteolysis Research Group, School of Biochemistry and Microbiology, University of Leeds, Leeds LS2 9JT, United Kingdom and the [§]Department of Biochemistry and Molecular Biology, Monash University, Melbourne, Victoria 3800, Australia*

**Angiotensin-converting enzyme-2 (ACE2) is a homologue of angiotensin-I converting enzyme (ACE), the central enzyme of the renin-angiotensin system (RAS). ACE2 is abundant in human kidney and heart and has been implicated in renal and cardiac function through its ability to hydrolyze Angiotensin II. Although ACE2 and ACE are both type I integral membrane proteins and share 61% protein sequence similarity, they display distinct modes of enzyme action and tissue distribution. This study characterized ACE2 at the plasma membrane of non-polarized Chinese hamster ovary (CHO) cells and polarized Madin-Darby canine kidney (MDCKII) epithelial cells and compared its cellular localization to its related enzyme, ACE, using indirect immunofluorescence, cell-surface biotinylation, Western analysis, and enzyme activity assays. This study shows ACE2 and ACE are both cell-surface proteins distributed evenly to detergent-soluble regions of the plasma membrane in CHO cells. However, in polarized MDCKII cells under steady-state conditions the two enzymes are differentially expressed. ACE2 is localized predominantly to the apical surface (~92%) where it is proteolytically cleaved within its ectodomain to release a soluble form. Comparatively, ACE is present on both the apical (~55%) and basolateral membranes (~45%) where it is also secreted but differentially; the ectodomain cleavage of ACE is 2.5-fold greater from the apical surface than the basolateral surface. These studies suggest that both ACE2 and ACE are ectoenzymes that have distinct localization and secretion patterns that determine their role on the cell surface in kidney epithelium and in urine.**

Angiotensin-I converting enzyme (ACE)[3] is a zinc metallopeptidase, which functions as a fundamental regulator of the renin-angiotensin system (RAS) by converting angiotensin I (Ang I) to the potent vasoconstrictor, angiotensin II (Ang II). ACE is an important target for the control of blood pressure and ACE inhibitors, being the primary treatment for hypertension, have been shown to have the broadest impact of any drug in cardiovascular medicine (1).

In 2000, a human homologue of ACE, angiotensin-converting enzyme-2 (ACE2), was independently identified by our group (2) and by others (3). ACE2 is an 805-amino acid protein that shares ~42% sequence identity to the N- and C-domains of somatic ACE (2). The predicted topology of ACE2 is that of a type I integral membrane protein consisting of a short C-terminal cytoplasmic domain (22 amino acids), a transmembrane domain anchoring ACE2 to the plasma membrane, and a large N-terminal ectodomain of 740 amino acids in which the catalytic zinc binding motif, HE*XX*H, is located. ACE2 functions exclusively as a carboxypeptidase (4, 5) and, therefore, differs in specificity from ACE, which can behave either as a peptidyl dipeptidase or an endopeptidase (6). ACE2 most efficiently cleaves apelin-13, dynorphin A (1–13), and des-Arg$^9$ bradykinin (4, 5). However, it is the ability of ACE2 to cleave the vasoconstrictor peptide Ang II to a putative cardioprotective metabolite, angiotensin (1–7) (Ang (1–7)) (7), which has implicated ACE2 as a potential regulator of the RAS (4, 5, 8, 9). The identification and characterization of ACE2 has uncovered an exciting new area of cardiovascular and renal physiology as well as providing possible therapeutic targets. Indeed, recent studies have shown that ACE2 mRNAs are altered in rat models of hypertension (10) and Type 1 and 2 diabetes (11, 12). The overexpression of ACE2 in cardiomyocytes (13) and studies of ACE2 in failing human hearts (8) and following myocardial infarction (14) all suggest that an up-regulation of ACE2 contributes to heart failure and ventricular remodeling. Furthermore, *ace2*$^{-/y}$ knock-out mice exhibit severe defects in cardiac contractility, which are restored by concomitant ACE ablation (10). These findings support the concept that ACE2 acts in a counter-regulatory manner to ACE and may play an important role to modulate the balance between vasoconstrictors and vasodilators in the kidney and heart. More recently, ACE2 has gained considerable attention as being a receptor for the coronavirus that causes severe acute respiratory syndrome (SARS) (15, 16) and as being protective against severe acute lung failure (17).

Although enormous focus has been placed on identifying and understanding the precise physiological roles for ACE2 in normal and disease states, the knowledge of the basic cell biology of ACE2 remains rudimentary. Specifically, there are no reports of the cellular targeting or sorting of ACE2 or ACE in polarized cells. Hence, the initial objective of this present study was to identify a human cell line of high endogenous ACE2 expression for cell biology studies. Following this our next approach was to employ Madin-Darby canine kidney type II (MDCKII) cells, a widely used polarized epithelial cell host for the expression and targeting of heterologous proteins. One of the highest areas of ACE2 and ACE expression is the kidney (2, 3, 18). MDCKII cells in culture retain many differentiated properties characteristic of kidney epithe-

* This work was supported in part by grants from the British Heart Foundation and the U.K. Medical Research Council (to A. J. T. and N. M. H.) and the Wellcome Trust (University of Leeds Bioimaging Suite). The costs of publication of this article were defrayed in part by the payment of page charges. This article must therefore be hereby marked "*advertisement*" in accordance with 18 U.S.C. Section 1734 solely to indicate this fact.

[1] Recipient of a C. J. Martin Research Fellowship awarded by the National Health and Medical Research Council (Australia).

[2] To whom correspondence should be addressed. Tel.: 44-113-343-3131; Fax: 44-113-242-3187; E-mail: a.j.turner@leeds.ac.uk.

[3] The abbreviations used are: ACE, angiotensin-I converting enzyme; ACE2, angiotensin-I converting enzyme 2; Ang, angiotensin; RAS, renin-angiotensin system; SARS, severe acute respiratory syndrome ; MDCKII, Madin-Darby canine kidney II; CHO, Chinese hamster ovary; HUVEC, human umbilical vein endothelial cell; RPTEC, renal proximal tubule epithelial cell; HCAECs, human coronary artery endothelial cell; SVSMC, saphenous vein smooth muscle cell; MES, 4-morpholineethanesulfonic acid; MBS, MES-buffered saline; GPI, glycosylphosphatidylinositol.

**TABLE ONE**

**Characteristics of primary antibodies used in this study**

| Target | Antibody | Immunogen | Source of ref. |
|---|---|---|---|
| ACE2 | | | |
| C-65 (cytoplasmic) | Polyclonal (rabbit) | Synthetic peptide amino acids 784–798 of human ACE2 protein | Pepceuticals, Ltd. (Leicester, UK) |
| Anti-hACE2$^{107}$ (extracellular) | Polyclonal (rabbit) | Synthetic peptide amino acids 107–116 of human ACE2 protein | (58) |
| ACE | | | |
| RH179 | Polyclonal (rabbit) | Recombinant protein amino acids 19–1306 of human ACE protein | (24) |
| MDCKII basolateral marker | | | |
| $Na^+/K^+$ ATPase $\alpha$1 subunit (M8-P1-A3) | Monoclonal (mouse) | Purified lamb kidney $\alpha$1 subunit | Sigma (Poole, UK) (catalog. no. A-277) |
| MDCKII apical marker | | | |
| gp135 mAb3F2 | Monoclonal (mouse) (hybridoma cell line 3F2) | gp135 | G. K. Ojakian (SUNY Downstate Medical Center) (26) |
| Lipid raft marker | | | |
| Caveolin-1 | Polyclonal (rabbit) | N-terminal of the human protein | BD Transduction Laboratories (catalog no. 610060) |

lium and, therefore, present an applicable cell line in which to study both ACE2 and ACE.

Thus, the present study has investigated the cellular localization and cell fate of ACE2 in comparison with ACE, an analogous protein to ACE2 both in sequence and membrane topology, in non-polarized Chinese Hamster Ovary (CHO) cells and polarized MDCKII cells. Furthermore, establishing an *in vitro* model of ACE2 and ACE expression in stably transfected polarized MDCKII cells provides a useful model to study the possible mechanisms regulating the cell fate and steady-state distribution of ACE2 and ACE in kidney epithelium.

## EXPERIMENTAL PROCEDURES

*Antibodies and Cell Culture*—The characteristics of the primary antibodies used are presented in TABLE ONE. Horseradish peroxidase-conjugated antibodies, donkey anti-rabbit and sheep anti-mouse and fluorescent-conjugated antibodies, goat anti-rabbit Alexa Fluor 488, and goat anti-mouse AlexaFluor 546, were purchased from GE Biosciences (UK) and Molecular Probes (Linden, The Netherlands), respectively. All cell lines (TABLE TWO) were obtained from the ECACC (Salisbury) unless otherwise specified and cultured according to their instructions (www.ecacc.org.uk). Human primary cultures of umbilical vein endothelial cells (HUVECs), renal proximal tubule epithelial cells (RPTECs, Clonetics) and coronary artery endothelial cells (HCAECs, PromoCell) were maintained according to the suppliers' instructions. Dr. K. E. Porter (University of Leeds) supplied human primary cultures of cardiac fibroblasts and saphenous vein smooth muscle cells (SVSMCs). EA.hy926 cells were a gift from Dr. C.-J. Edgell (University of North Carolina).

*Reverse Transcription-PCR—ACE2* gene expression in cell lines was determined using a Titanium$^{TM}$ one-step reverse transcriptase-PCR kit according to the manufacturer's protocol and thermal profile (BD Biosciences). Total RNA was isolated from human cells using TRIzol (GE Biosciences). cDNA was generated using *ace2* gene-specific primers and then amplified by PCR using the same primers (forward: 5′-GCTTCAGCTGCAGGCTCTTCAGC-3′; reverse: 3′-GCAAATCAGCAGGGAGGCATCC-5′). Glyceraldehyde-3-phosphate dehydrogenase cDNA (internal control) was amplified from each cell line using specific primers (forward: 5′-TGAAGGTCGGAGTCAACGGATTTGGT-3′; reverse: 5′-CATGTGGGCCATGAGGTCCACCAC-3′). The products were visualized on a 2% agarose gel stained with ethidium bromide. PCR products were verified by DNA sequencing (Lark Technologies).

*Preparation of Cell Membranes*—Confluent cells were washed twice in phosphate-buffered saline and scraped from culture flasks into 50 mM Hepes containing 20 mM $CaCl_2$ and EDTA-free inhibitor mixture (Roche Applied Science, pH 7.5). Cells were lysed using a Parr cell disruption bomb using $N_2$ (800 p.s.i. at 4 °C) for 10 min, and the lysates were centrifuged at 100,000 × *g* for 1 h. The resultant membrane pellet was resuspended in enzyme buffer (50 mM Hepes, 200 mM NaCl, 10 $\mu$M $ZnCl_2$ (pH 6.8), and 1% Triton (v/v) X-100). Protein concentration was determined by the bicinchoninic acid method (Sigma), using bovine serum albumin as standard.

*Quenched Fluorescent Substrate Activity Assays*—The activities of ACE2 and/or ACE in cell membrane preparations generated from human cell lines, the media from secretion studies, and human urine were determined as the breakdown of 50 $\mu$M fluorogenic substrate (ACE2, ((7-methoxycoumarin-4-yl)acetyl-Ala-Pro-Lys-(2,4-dinitrophenyl)-OH or ACE, ((7-methoxycoumarin-4-yl)acetyl-Ala-Ser-Asp-Lys-(2,4-dinitrophenyl)-L-2,3-diaminopropionyl)), by either 50 $\mu$g of total protein of cell membrane preparation, 50 $\mu$g of total protein of media, or 50 $\mu$l of urine. All experiments were performed as described previously (4). Specific activities of ACE2 and ACE were determined using the inhibitors 200 $\mu$M Pro-Phe (5), or 100 nM MLN4760 (19) for ACE2, and 10 $\mu$M captopril or ramipril for ACE. Purified soluble ACE2 (R & D Systems) or purified pig ACE was used to determine the amount of fluorescence generated per nanogram of substrate hydrolyzed per milligram of protein. Human urine analyzed for ACE2 specific activity was collected from 6 normal patients of both genders, aged 23–55 years, that were not suffering hypertension, renal complication, or any related disorder.

*cDNA Constructs*—The cDNA corresponding to the full-length ACE2 coding sequence was isolated from a kidney cDNA library, amplified by PCR, and subcloned into the XbaI/XhoI sites of the pCINeo mammalian expression vector (Promega). The cDNA encoding full-length human somatic *ace* was a gift from Prof. P. Corvol (INSERM,

Paris, France) and subcloned into pIRESNeo (Clontech Laboratories Inc.) (20).

*Expression of ACE2 and ACE in CHO and MDCKII Cells*—All transient transfections were performed as previously described (2). To establish stable expression, cells were split at a ratio of 1:50 72 h after the start of transfection and selected for using G418 (CHO, 1 mg $ml^{-1}$; MDCKII, 0.5 mg $ml^{-1}$). FACScan with CELLQUEST software (BD Biosciences) was employed to differentiate MDCKII cells of high or low protein expression levels and normal morphology as previously described (21). The transepithelial electrical resistance of MDCKII monolayers grown on Transwell filters (Corning Costar, 3412 and 3460, pore size 0.4 $\mu$m) for biotinylation and immunofluorescence studies was measured using a Millicell-ERS Voltohmmeter (Millipore, Bedford, MA) to assess the integrity of tight junctions. All experiments were performed at an electrical resistance of $>200\ \Omega\ cm^{-2}$.

*SDS-PAGE and Immunoblotting*—Proteins were resolved by SDS-PAGE by using 6% or 7–17% gradient polyacrylamide gels and transferred onto Immobilon P polyvinylidene difluoride membranes in a Tris-glycine buffer with 10% (v/v) methanol and 0.04% (w/v) SDS. The membrane was saturated with Tris-buffered saline (pH 7.5) containing 10% (w/v) nonfat milk for 1 h at 37 °C, then incubated overnight at 4 °C with primary antibody. Horseradish peroxidase-conjugated secondary antibodies (GE Biosciences) were used at 1:4,000, and bound antibodies were detected by using a enhanced chemiluminescence system (GE Biosciences).

*Enzymatic Deglycosylation*—*N*-Glycosidase F deglycosylation of cell membrane preparations was performed according to the supplier's instructions (New England BioLabs, Inc.).

*Cell-surface Biotinylation of Non-polarized Cells*—All stages of the procedure were performed at 4 °C and as previously described (22). Cells were washed with ice-cold phosphate-buffered saline (containing 1 mM $CaCl_2$ and 1 mM $MgCl_2$). Cells were biotinylated using 5 ml of 2 mg/ml biotinamidocaproate *N*-hydroxysuccinimide ester constituted in 40 mM bicarbonate buffer (pH 8.6) for 30 min. Cells were subsequently lysed with 0.5 ml of radioimmune precipitation assay buffer (pH 8.0) consisting of 50 mM, Tris, 150 mM NaCl, 1% (v/v) Nonidet P-40, 0.5% (v/v) deoxycholic acid, 0.1% (v/v) SDS, and EDTA-free complete protease inhibitor mixture (Roche Applied Science). The collected lysate (1 mg/ml) was centrifuged at 10,000 × *g* for 30 min to pellet debris, and the pellet was retained for analysis. The clear lysate was rotated for 2 h with 200 $\mu$l of streptavidin-agarose beads suspended in 0.01 M $NaPO_4$, 0.15 M NaCl (pH 7.2). The beads were recovered by centrifugation for 1 min at 10,000 × *g* and washed twice in phosphate-buffered saline using rotation and centrifugation. Samples were prepared for immunoblotting by resuspending the pellet and streptavidin-agarose beads in 4× Laemmli sample buffer or by precipitating the supernatant containing cytosolic proteins with 10% (w/v in acetone) trichloroacetic acid on ice, sedimenting by centrifugation at 4 °C for 10 min at 12,000 × *g*, washing twice with acetone, and resuspending in 4× Laemmli sample buffer.

*Cell-surface Biotinylation of Polarized Cells Grown on Transwell Filters*—Biotinylation was performed as described above, using biotinamidocaproate *N*-hydroxysuccinimide ester constituted in 40 mM bicarbonate buffer (pH 7.5). Cells were grown on polycarbonate Transwell filters (Costar 3412), and biotin was added to either the apical or basolateral, or both compartments. The opposite compartment (without biotin) was filled with phosphate-buffered saline and 1% (w/v) bovine serum albumin. Cells were subsequently lysed and biotinylated protein was affinity-precipitated as described above. The biotinylated proteins were eluted from beads using 50 $\mu$l of Laemmli sample buffer at 100 °C for 5 min.

*Uptake Studies*—Biotinylation studies were performed as previously described (22) using membrane-impermeable, thiol-cleavable EZ-link-NHS-SS-Biotin (sulfosuccinimidyl 2-(biotinamido)ethyl-1,3-dithiopropionate, Pierce). To allow re-internalization, cells were incubated with complete medium containing 10% (v/v) fetal calf serum at 37 °C for various times. Cells were washed three times for 15 min each with glutathione buffer (50 mM glutathione (reduced), 90 mM NaCl, 1.25 mM $CaCl_2$, 1.25 mM $MgSO_4$, 0.2% (w/v) bovine serum albumin, pH 8.6). Cells were lysed and the biotin-labeled protein affinity-precipitated as described in the section above. Protein levels were quantified by densitometry (Luminescent Image Analyzer LAS-1000 plus and Imaging Reader version 2.3 software, Fuji Photofilm Co. Ltd.).

*Immunofluorescence and Microscopy*—Transfected CHO cells expressing full-length ACE2 or ACE were cultured on glass coverslips overnight prior to fixation using 4% (w/v) paraformaldehyde (Sigma) for 10 min at 37 °C. The reactive aldehyde groups were quenched by 50 mM $NH_4Cl$ for 15 min at 25 °C, and cells were permeabilized using Triton X-100 for 5 min at 25 °C. Nonspecific binding was blocked using 0.2% (w/v) gelatin and 1% (v/v) normal goat serum (Sigma) for 30 min at 25 °C prior to immunostaining with primary antibody for 2 h at 25 °C. Alternatively, MDCKII cells expressing full-length ACE2 or ACE were cultured on Transwell filters for 7 days, then blocked for nonspecific binding as above, followed by incubation with primary antibody for 3 h at 4 °C at either the apical or basolateral surface. Cells were then fixed using 4% (w/v) paraformaldehyde (Sigma) for 10 min at 37 °C and the reactive aldehyde groups quenched by 50 mM $NH_4Cl$ for 15 min at 25 °C. Application of the secondary antibody was the same for both CHO cells and MDCKII cells. Cells were incubated with the appropriate fluorescent-conjugated secondary antibodies for 30 min at 25 °C. Coverslips or Transwell filters were mounted in Vectashield and viewed using a ×63/1.4 numerical aperture oil immersion objective lens on a Zeiss Axioplan 2 imaging microscope (Carl Zeiss, Ltd.). Confocal laser scanning microscopy was performed using a Zeiss LSM510 confocal scan module. Data were processed by using LSM software (Zeiss, Jena, Germany) and transferred to Adobe Photoshop version 6.0 for reproduction.

*Isolation of Detergent-insoluble Membrane Domains*—All steps were carried out at 4 °C. Confluent cells were scraped into 2 ml of 2-morpholino-ethanesulfonic acid (MES)-buffered saline (MBS, 25 mM MES, 0.15 M NaCl, pH 6.5) containing 1% (v/v) Triton X-100 and resuspended by passing 5 times through a 25-gauge needle. An equal volume of 90% (w/v) sucrose in MBS was added, and 1-ml aliquots were placed in 5-ml ultracentrifuge tubes; 4-ml discontinuous sucrose gradients consisting of 35% (w/v) sucrose in MBS (2 ml) and 5% (w/v) sucrose in MBS (2 ml) were layered on top. The sucrose gradients were centrifuged at 100,000 × *g* for 18 h at 4 °C in a Beckman SW55 rotor, and fractions (0.6 ml) were harvested from the bottom to the top of the tube.

*Secretion of Soluble ACE2 and ACE from Polarized Cells*—Serum-free medium (Opti-Mem™, Invitrogen) was added to cells (1.5 ml apical and 2.6 ml basolateral of the monolayer) and collected after various time points (0.5, 1, 3, 6, 16, and 24 h). The volume of the apical medium sample was adjusted to 2.6 ml with Opti-Mem. Media samples were concentrated to a 500-$\mu$l volume by centrifugation using size exclusion Vivaspin 5-ml concentrators (10,000 molecular weight cutoff). Media (50 $\mu$g of total protein) were analyzed for specific ACE2 or ACE activity using quenched fluorescent substrate assays. To study the action of potential sheddases involved in ACE2 and ACE secretion, the effect of the shedding inhibitors, Ilomastat (GM6001, 25 $\mu$M, Chemicon Inter-

national) and TAPI-2 (10 $\mu$M, Peptide International) was examined. Cells were incubated in the absence and presence of Ilomastat for 3 h. One-way analysis of variance followed by Bonferroni post-hoc analysis was used to compare data (Prism version 3.0, GraphPad Software). $p < 0.05$ was considered significant.

## RESULTS

*Endogenous Expression of ACE2 in Human Cell Cultures*—Human cell lines and primary cultures of cardiac, vascular, renal, and gastrointestinal origin were screened by reverse transcriptase-PCR and by quenched fluorescent substrate assay for the endogenous expression of ACE2. Primer-specific amplification of a 500-bp PCR product derived from total RNA encoding the *ACE2* gene transcript was visible in all cell lines but very faint for ACHN and HEK cell lines where gene expression was low (Fig. 1). To investigate if the transcript observed in cell lines was translated into a catalytically active protein, cell membrane fractions were isolated from human cell cultures. Solubilized membrane fractions were incubated with the ACE2 fluorogenic substrate ((7-methoxycoumarin-4-yl)acetyl-Ala-Pro-Lys-(2,4-dinitrophenyl)-OH) as previously described (4, 5). ACE2 hydrolysis of this substrate occurs between the proline and lysine residues. The specificity of the ACE2 activity was determined using the dipeptide Pro-Phe (200 $\mu$M), which completely inhibits ACE2 activity at 180 $\mu$M (5). For comparative purposes, activity assays were performed in parallel using the ACE-specific fluorogenic substrate ((7-methoxycoumarin-4-yl)acetyl-Ala-Ser-Asp-Lys-(2,4-dinitrophenyl)-L-2,3-diaminopropionyl)). The specificity of ACE activity was confirmed using the ACE inhibitor, captopril (10 $\mu$M). Overall, the endogenous expression of ACE2 activity was 15- to 50-fold lower than that observed for ACE. The highest levels of expression for ACE2 and ACE were observed in the primary cultures of RPTECs, HUVECs, cardiac fibroblasts, SVSMCs, and HCAECs (TABLE TWO). There was not a consistent correlation between *ACE2* gene expression and ACE2 proteolytic activity in the cell lines screened. This finding is in keeping with a recent observation that ACE2 gene and protein expression is mismatched in some tissues in rats and mice (23).

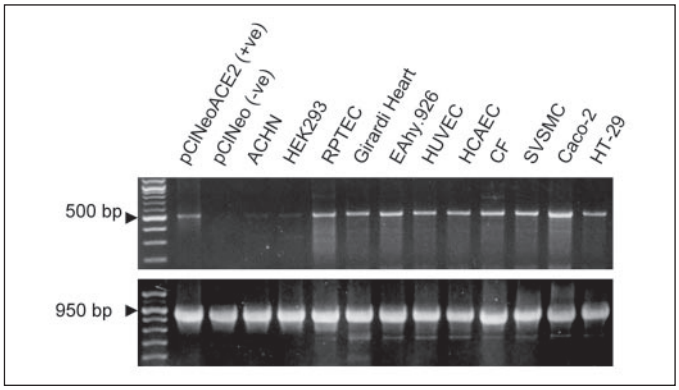


FIGURE 1. **ACE2 and glyceraldehyde 3-phosphate dehydrogenase primer-specific amplification of cDNA reverse-transcribed from total RNA originating from human cell lines and primary cultures.** The amplicons (ACE2, 500 bp and GADPH, 950 bp) were separated and visualized on a 2% (w/v) agarose gel stained with ethidium bromide. Total RNA used for reverse transcriptase-PCR controls was derived from CHO cells transfected with cDNA encoding full length ACE2 subcloned into pCINeo (positive control) or the empty vector (negative control).

*Recombinant Expression of ACE2 and ACE in CHO Cells*—Because endogenous levels of ACE2 were too low to allow direct biochemical and cellular analysis using our antibodies in Western blotting and immunoprecipitation, we stably transfected CHO cells with cDNA encoding full-length ACE2. In parallel, a CHO cell line expressing full-length somatic ACE was also created. ACE2 expressed in CHO cells was detected as a single ~120-kDa polypeptide in solubilized membrane preparations and in the conditioned medium after 16 h by Western blotting using the polyclonal antibody anti-hACE2[107] directed to the extracellular domain of ACE2 (Fig. 2*A*). Soluble ACE2 was not detected in conditioned medium using the cytoplasmic antibody, C-65 (data not shown). No reactivity was observed in untransfected cells or in cells overexpressing ACE (data not shown). The polyclonal anti-ACE antibody RH179 detected a ~180-kDa band in the solubilized membrane preparation and in the media collected from CHO cells stably expressing ACE (Fig. 2*B*).

*ACE2 Is a Cell-surface Protein*—Indirect immunofluorescence was used to visualize the cellular localization of ACE2 in non-polarized CHO cells. In CHO cells, ACE2 was localized to the cell surface (Fig. 2*C*). Little intracellular staining was observed in permeabilized paraformaldehyde-fixed cells (Fig. 2*C*). ACE stably expressed in CHO cells was also localized to the cell surface, in agreement with our previous finding (Fig. 2*C*) (22).

To further confirm the cell-surface location of ACE2, we employed direct biotinylation. CHO cells expressing ACE2 or ACE were biotiny-

**TABLE TWO**

**The specific activities of ACE2 and ACE in human transformed cells and primary cell cultures**

The activities of ACE2 and ACE in each of the cell lines were determined as the formation of product (Mca) from the breakdown of 50 $\mu$M fluorogenic substrate. Specificity for ACE2 and ACE was determined using 200 $\mu$M Pro-Phe and 10 $\mu$M captopril, respectively. Values represent the mean ± S.E. of three independent experiments performed in duplicate.

| Human cell | Origin | ACE2 | ACE |
|---|---|---|---|
| | | *ng/mg enzyme* | |
| Transformed cells | | | |
| ACHN | Renal adenocarcinoma | 2.54 ± 0.24 | 25.76 ± 4.55 |
| HEK293 | Embryonic kidney | 2.28 ± 0.55 | 29.79 ± 0.51 |
| Girardi heart | Heart | 9.49 ± 1.47 | 34.85 ± 3.15 |
| Eahy.926 | Hybrid HUVEC/A549 | 2.92 ± 1.59 | 81.31 ± 6.79 |
| CACO-2 | Colon carcinoma | 2.05 ± 0.28 | 38.89 ± 5.95 |
| HT-29 | Colon adenocarcinoma | 2.49 ± 0.26 | 14.64 ± 3.31 |
| Primary cultures | | | |
| RPTECs | Renal proximal tubule | 23.06 ± 2.40 | 175.90 ± 7.92 |
| HUVECs | Umbilical vein | 13.94 ± 0.99 | 652.80 ± 23.67 |
| HCAECs | Coronary artery | 9.60 ± 0.97 | 398.67 ± 22.05 |
| CF | Cardiac fibroblast | 15.61 ± 3.75 | 157.07 ± 55.70 |
| SVSMCs | Saphenous vein | 11.53 ± 0.82 | 171.55 ± 48.92 |

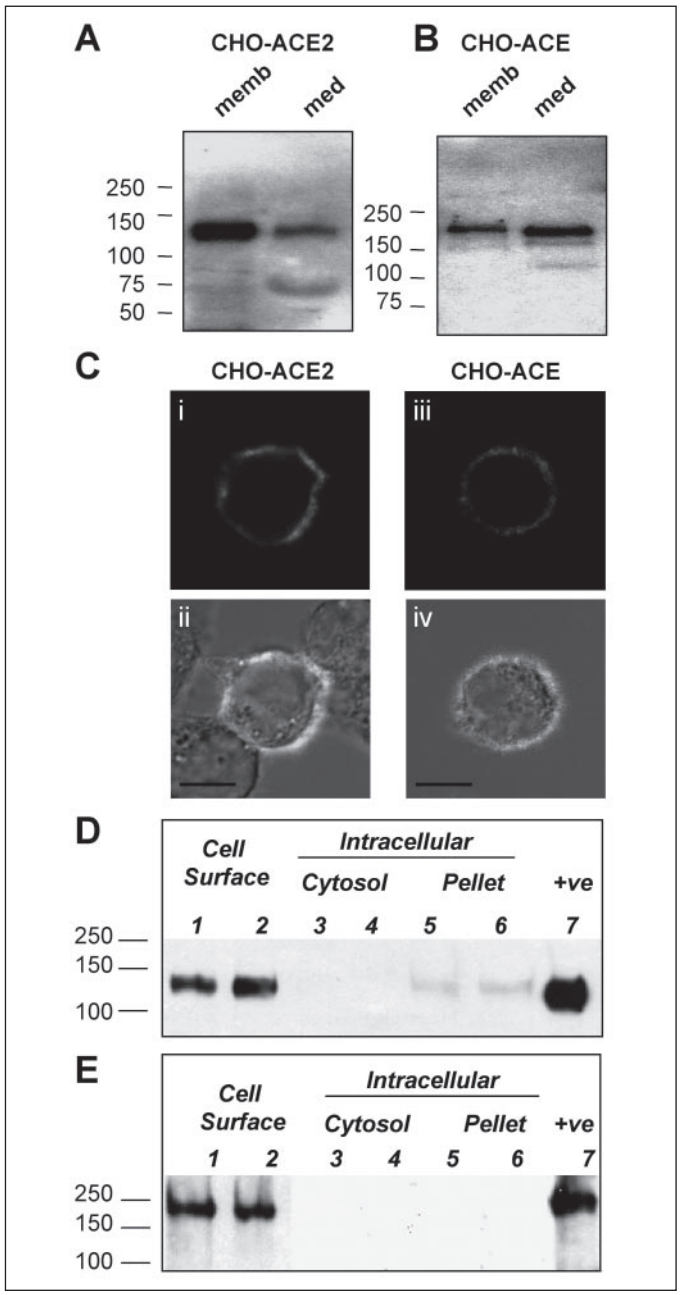


FIGURE 2. Transient expression of ACE2 (*A*) and ACE (*B*) in CHO cells. ACE2 and ACE were separated on a 6% gel and detected in solubilized cell membranes (*memb*) (30 $\mu$g) and in the conditioned media (*med*) (100 $\mu$g). *C*, cell surface localization of ACE2 and ACE expressed in CHO cells by immunofluorescent staining. Cells grown on coverslips were fixed using 4% paraformaldehyde, permeabilized with 0.02% Triton X-100 and immunostained with N-terminal anti-hACE2[107] antibody (1:100) (*i*) or RH179 anti-ACE (1:100) (*iii*). Cells were viewed using differential interference contrast (*ii* and *iv*) and immunofluorescence confocal microscopy. Donkey anti-rabbit Alexa Fluor 488 (1:400) was used as secondary. *Bar*, magnification 63× (6 $\mu$m). Immunoblots of biotinylated cell-surface proteins in CHO cells stably transfected with ACE2 (*D*) and ACE (*E*). Cells were biotinylated and lysed, of which 30 $\mu$g of protein was immunoprecipitated on streptavidin-agarose beads. *Lanes 1* and *2*, biotinylated protein retained on streptavidin-agarose; *lanes 3* and *4*, the trichloroacetic acid immunoprecipitated supernatant containing non-biotinylated proteins (soluble cytosolic protein fraction); *lanes 5* and *6*, cell lysate membrane pellet. *Lane 7*, positive (+*ve*) controls of purified human ACE2 (10 ng) or purified human somatic ACE (10 ng). Immunoblots were probed using antibodies directed to ACE2 (C-65) and ACE (RH179).

lated using biotinamidocaproate *N*-hydroxysuccinimide ester. Both ACE2 and ACE were detected in their respective biotinylated protein fractions, with little or no ACE2 or ACE present in the soluble protein fraction (Fig. 2, *D* and *E*). A low level of ACE2 was detected in the cell lysate pellet, which may represent ACE2 in membranes from secretory organelles such as the endoplasmic reticulum or Golgi (Fig. 2*D*).

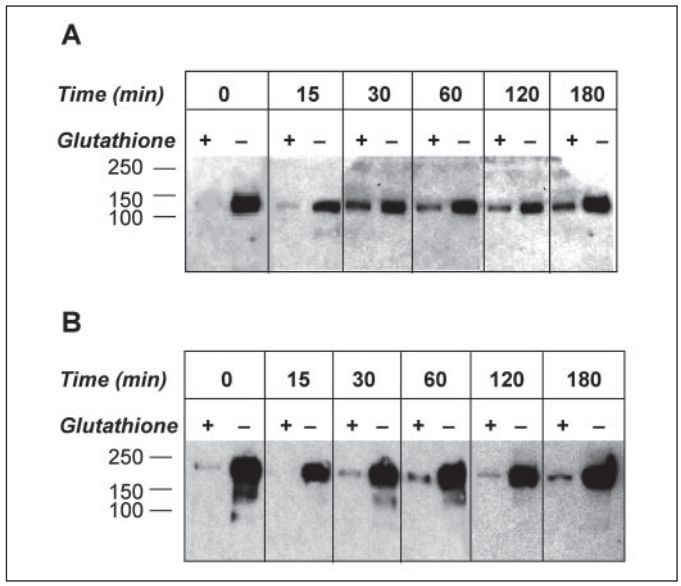


FIGURE 3. **Internalization of cell surface-located ACE2 (*A*) and ACE (*B*).** The internalization of protein was analyzed by incubating cells at 37 °C after biotinylation. At the time points indicated cells were treated with glutathione buffer (+) or left untreated (−). Biotinylated proteins were precipitated with streptavidin-conjugated agarose beads and eluted in SDS-PAGE sample loading buffer. ACE2 and ACE were detected by Western immunoblotting using anti-hACE2[107] and RH179 antibodies, respectively.

*Internalization of ACE2 and ACE in CHO Cells*—To investigate if ACE2 and ACE are re-internalized from the plasma membrane, cell-surface proteins were coupled to the membrane-impermeable covalent linker EZ-link-NHS-SS-biotin and then returned to media supplemented with 10% fetal calf serum at 37 °C, for up to 180 min. At 0, 15, 30, 60, 120, and 180 min, EZ-link-NHS-SS-Biotin label was cleaved from proteins by the reducing agent, glutathione, at 4 °C. Under these conditions, EZ-link-NHS-SS-Biotin can be selectively removed from those proteins localized at the cell surface, whereas any internalized proteins retain their biotin label. Over the period of 180 min less than 24% of ACE2 was internalized compared with uncleaved controls (Fig. 3*A*). A similar internalization pattern was observed for ACE with only ~13% internalization occurring after 180 min (Fig. 3*B*). The observation that ACE2 and ACE do not readily internalize from the cell surface is consistent with our hypothesis that ACE2, like ACE, has a role at the cell surface in metabolizing circulating peptides.

*ACE2 and ACE Are Not Raft-localized in CHO Cells*—Lipid rafts are domains within the plasma membrane that are rich in sphingolipids, cholesterol, GPI-anchored, and acylated proteins. These domains are thought to be important in membrane signaling and trafficking events. Rafts are biochemically characterized by their insolubility in non-ionic detergents, most commonly Triton X-100 at 4 °C (25). Both ACE2 and ACE expressed in CHO cells were predominantly soluble in Triton X-100 at 4 °C when separated by buoyant sucrose density gradient centrifugation (Fig. 4, *A* and *B*). Relatively little or no ACE2 or ACE were observed to be associated with lipid rafts or caveolae, given the absence of any co-localization with the caveolae/lipid raft marker, caveolin-1, which is found in detergent-insoluble glycolipid-enriched fractions (fractions 4–6) of the cell membrane (Fig. 4, *A* and *B*).

*Expression of ACE2 and ACE in MDCKII Cells*—Three individual MDCKII cell lines expressing different levels of ACE2 (designated cell lines 10, 27, and 36) or ACE (designated cell lines 5, 22, and 7) were selected (Fig. 5). In addition to a high expressing line, two low or

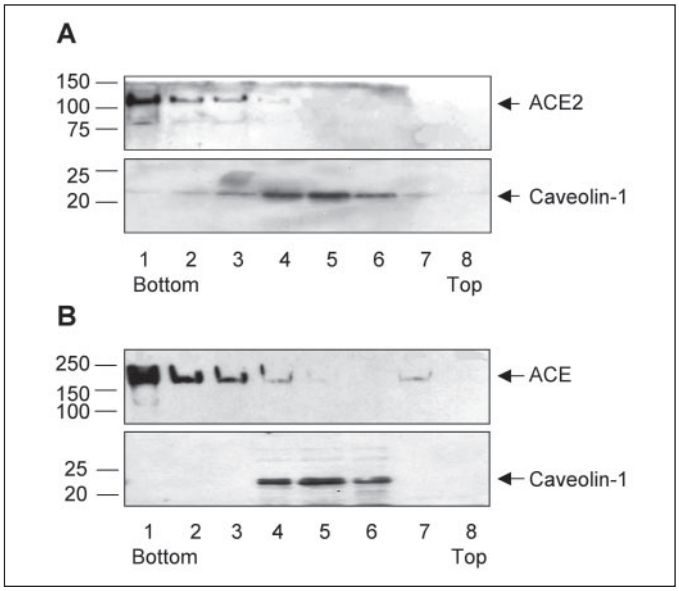


FIGURE 4. **Isolation of lipid rafts from CHO cells stably expressing ACE2 (*A*) or ACE (*B*).** Lipid rafts were isolated from cells stably expressing ACE2 or ACE. Sucrose gradients were harvested in 0.6-ml fractions (*fraction 1*, *bottom* of gradient; *fraction 8*, *top* of gradient), and each fraction was analyzed by SDS-PAGE and immunoblotted with polyclonal antibodies, anti-ACE2 C-65, anti-ACE RH179, or anti-caveolin-1.

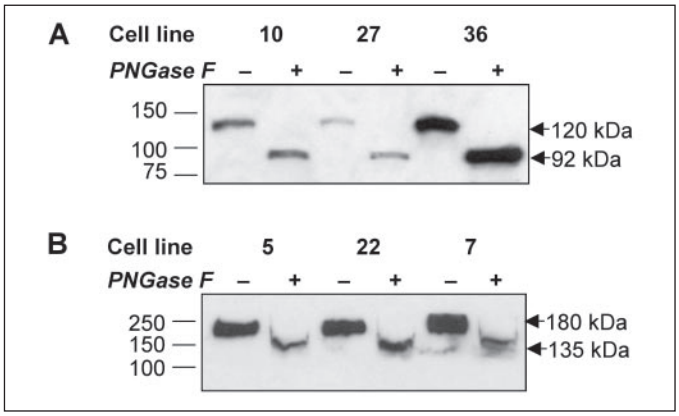


FIGURE 5. **Expression of ACE2 and ACE in MDCKII transfected cell lines.** *N*-Deglycosylation of ACE2 (*A*) and ACE (*B*). Cell membranes (30 $\mu$g) of MDCKII cells stably expressing ACE2 or ACE were treated with (+) and without (−) peptide *N*-glycosidase F. ACE2 and ACE were detected by Western immunoblotting using anti-hACE2[107] and RH179 antibodies, respectively.

medium lines were selected to ensure saturation of polarized sorting was avoided. Individual cell lines were selected using cloning discs from neomycin-resistant cells that had been growing for 2 weeks. These individually selected cell lines were then sorted using a fluorescence-activated cell sorter to obtain a homogeneous population. Expression of a fully glycosylated protein by each cell line was verified by deglycosylating solubilized membranes using peptide *N*-glycosidase F for 4 h at 37 °C. In MDCKII-ACE2 cell lines, low expressing cell lines 10 and 27 and high expressing cell line cell line 36, a single ~120-kDa protein band was observed. This ~120-kDa band migrated to ~92 kDa upon deglycosylation by peptide *N*-glycosidase F (Fig. 5*A*).

Three MDCKII-ACE cell lines were selected: cell lines 5, 22, and 7. For each cell line, a single ~180-kDa protein band was detected in solubilized membrane preparations using polyclonal anti-ACE antibody RH179. Upon deglycosylation, the ACE produced by each cell line migrated to ~135 kDa (Fig. 5*B*).

*ACE2 Is Targeted Predominantly to the Apical Surface, whereas ACE Is Delivered to Both the Apical and Basolateral Surfaces*—To determine the surface distribution of ACE2 and ACE, the MDCKII cells described above were grown on Transwell filters to form polarized monolayers. In immunofluorescence studies, ACE2 antibody anti-hACE2[107] or ACE antibody RH179 was incubated on either the apical or basolateral surfaces of the monolayer. Antibodies directed to the well characterized endogenous apical and basolateral surface markers, gp135 (26) and $Na^+/K^+$ ATPase ($\alpha$1 subunit) (27), respectively, were used in co-localization studies. Confocal microscopy revealed ACE2 was targeted almost exclusively to the apical surface. This was also confirmed by analyzing vertical cross sections (*z*-axis) of polarized monolayers (Fig. 6, *A* and *B*). Strong co-localization of ACE2 with apical glycoprotein gp135 was observed (Fig. 6*C*). Very weak staining was observed for ACE2 on basolateral membranes (Fig. 6*D*) compared with the strong staining observed for endogenous $Na^+/K^+$ ATPase ($\alpha$1 subunit) (Fig. 6*E*). The correct localization of surface markers, gp135 and $Na^+/K^+$ ATPase ($\alpha$1 subunit) to the apical and basolateral membranes of MDCKII cells, respectively, suggests cell trafficking was unaltered by overexpression of ACE2.

In concurrent experiments, direct biotinylation was performed. Cells were biotinylated on either separate cell surface (apical or basolateral) or on both sides. Surface-biotinylated ACE2 was detected by immunoblotting using antibody anti-hACE2[107]. This technique also revealed ACE2 to be targeted predominantly to the apical surface (Fig. 6*G*). Quantification by densitometry of multiple experiments with three individual cell lines revealed that 91.9 ± 1.8% ($n = 3$) of ACE2 is targeted to the apical surface, whereas only 8.1 ± 1.9% ($n = 3$) was on the basolateral side (Fig. 6*H*).

In comparison, indirect immunofluorescent studies of MDCKII-ACE cell lines revealed ACE was present on both the apical and basolateral cell surfaces (Fig. 7, *A* and *D*). Immunofluorescent staining of ACE was stronger on the apical surface than on the basolateral surface. Confocal images of ACE showed co-localization with gp135 on the apical surface (Fig. 7, *B* and *C*) and $Na^+/K^+$ ATPase ($\alpha$1 subunit) on the basolateral surface (Fig. 7, *E* and *F*). In immunofluorescence studies, direct biotinylation of monolayers revealed ACE was distributed to both surfaces, with 58.7 ± 2.3% ($n = 3$) being targeted to the apical surface and 41.0 ± 2.4% ($n = 3$) of ACE to the basolateral surface (Fig. 7, *G* and *H*). For all ACE2 and ACE biotinylation experiments, parallel gels were run using the same samples and probed using an antibody to the basolateral marker $Na^+/K^+$ ATPase ($\alpha$1 subunit). $Na^+/K^+$ ATPase ($\alpha$1 subunit) was observed exclusively in the basolateral and total (apical plus basolateral) biotin-labeled fractions confirming equal loading and that the integrity of the monolayer was maintained during the biotinylation process (Figs. 6*G* and 7*G*).

*Secretion of ACE2 and ACE*—To investigate if secretion has a role in establishing or maintaining a polarized distribution of ACE2 and ACE in MDCKII cells, medium was collected from the apical and basolateral compartments of MDCKII monolayers, grown on Transwell filters, over a period of 24 h. At each time point the enzymatic activity of media collected from each compartment and the monolayer cell lysate were tested by quenched fluorescent substrate assay. Secretion of ACE2 and ACE from intact monolayers was cumulative and time-dependent. At time points 0.5, 1, 3, 6, 16, and 24 h, the level of ACE2 activity secreted from the apical surface was at least 5-fold greater (87 ± 1.3% apical, $n =$ 3) than that secreted from the basolateral side at each time interval (Fig. 8*A*). In comparison, ACE activity in media collected from the apical side was 2.3- to 3.4-fold greater (71 ± 2.9% apical, $n = 3$) than that from the basolateral side (Fig. 8*B*). Over the 24-h time period, no significant

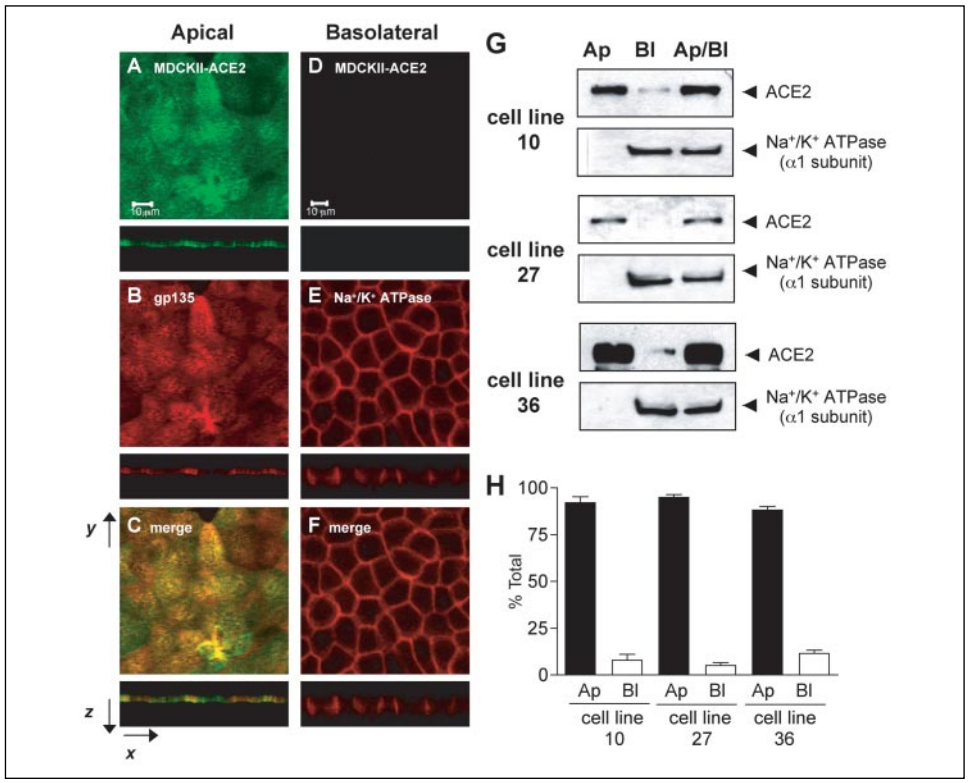


FIGURE 6. **Cellular localization of ACE2 in polarized MDCKII cells.** Immunofluorescent staining of ACE2 (cell line 36), gp135 (apical marker), and $Na^+/K^+$ ATPase ($\alpha$1 subunit) (basolateral marker). ACE2 (*A*) co-localizes with endogenous apical marker gp135 (*B* and *C*) but not basolateral marker ($Na^+/K^+$ ATPase ($\alpha$1 subunit) (*E* and *F*). Cell-surface biotinylation of ACE2 low (cell lines 10 and 27) and high (cell line 36) expressing cell lines (*G*). Biotinylated surface proteins (pH 7.5) were isolated using streptavidin-coated agarose beads. Surface-biotinylated ACE2 molecules (120 kDa) were detected by immunoblotting using antibody anti-hACE2[107] and quantified by densitometry (*H*). The same samples were separated on parallel gels and immunoblotted for $Na^+/K^+$ ATPase ($\alpha$1 subunit) (110 kDa) using M8-P1-A3 antibody. Note: $Na^+/K^+$ ATPase ($\alpha$1 subunit) was observed exclusively in the basolateral biotin-labeled protein fraction. Data shown are mean ± S.E. of three independent experiments.

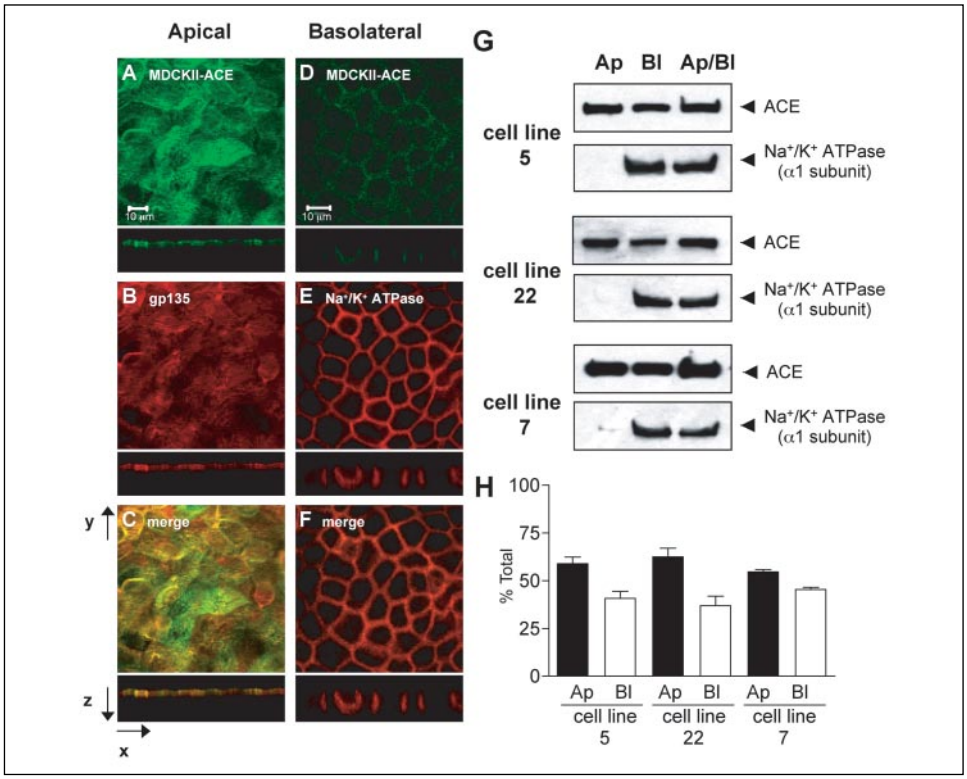


FIGURE 7. **Protein sorting of ACE in polarized MDCKII cells.** Indirect immunofluorescent staining of ACE (cell line 7) to both the (*A*) apical and (*D*) basolateral cell surface. Colocalization of ACE with endogenous (*B* and *C*) apical (gp135) and (*E* and *F*) basolateral ($Na^+/K^+$ ATPase $\alpha$1 subunit) surface markers are shown. Cell-surface biotinylation of ACE (180 kDa) (cell lines 5, 22, and 7) expressing cell lines (*G*). Biotinylated surface proteins (pH 7.5) were isolated using streptavidin-coated agarose beads. Surface-biotinylated ACE molecules were detected by immunoblotting using antibody RH179 (180 kDa) and quantified by densitometry (*H*). The same samples were separated on parallel gels and immunoblotted for $Na^+/K^+$ ATPase ($\alpha$1 subunit) (110 kDa) using M8-P1-A3 antibody. Data shown are mean ± S.E. of three independent experiments.

change of activity was observed in cell lysates from cells expressing ACE2 or ACE (data not shown). Because the secretion of ACE and other integral membrane proteins is mediated by metalloproteases (sheddases), the effect of metallosheddase inhibitors, Ilomastat (25 $\mu$M) and TAPI-2 (10 $\mu$M), on ACE2 and ACE secretion was studied. Ilomastat significantly inhibited the apical secretion of ACE2 by 43.8 ± 0.96% ($p <$ 0.01, $n = 3$) after 3 h incubation. The low level of ACE2 basolateral secretion (< 13%) was unaltered by Ilomastat. Comparatively, Ilomastat (25 $\mu$M) significantly inhibited ACE secretion on the basolateral surface of MDCKII cells (% inhibition *versus* untreated: basolateral 54.7 ± 0.33, $p < 0.01$, $n = 3$) but not the apical surface (% inhibition *versus* untreated: apical 15.3 ± 0.88, $p > 0.05$, $n = 3$). The secretion of ACE from both the

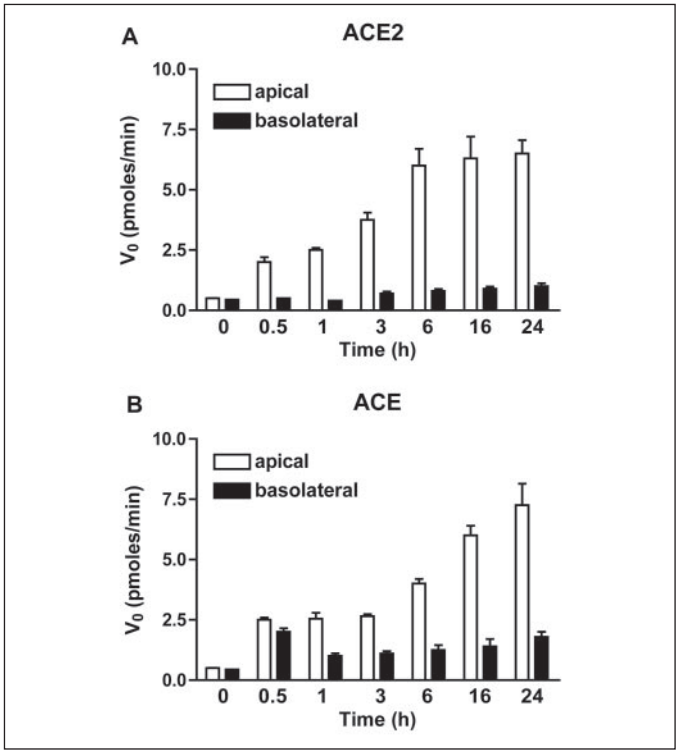


FIGURE 8. **Ectodomain shedding of ACE2 and ACE.** Time course of activity of (*A*) ACE2 (clone 36) and (*B*) ACE (clone 7) from media collected from the apical and basolateral cell surfaces of transfected MDCKII cells over a 24-h period. Three to four independent experiments were performed in duplicate. Parallel experiments were performed with non-transfected MDCKII cells to determine nonspecific activity.

apical and basolateral surface of MDCKII cells was significantly reduced by TAPI-2 (10 $\mu$M) (% inhibition *versus* untreated: apical 45.9 $\pm$ 8.03 $p <$ 0.01, $n = 3$; basolateral 82.4 $\pm$ 1.03, $p < 0.01$, $n = 3$). TAPI-2 did not significantly inhibit the secretion of ACE2.

*Human Urine*—Quenched fluorescent ACE2 specific activity was measured in human urine from six healthy individuals (3 males and 3 females 23–53 years of age) using the selective ACE2 inhibitor, MLN4760. The mean net activity (the difference between levels in the presence and absence of ACE2 inhibitor, MLN4760) was 34.3 $\pm$ 5.57 pmol of substrate hydrolyzed/ml/min and was equivalent to 1179 $\pm$ 213 pg of ACE2/ml. In contrast, ~10-fold less specific ACE activity was detected in urine compared with the observed ACE2 activity using an ACE quenched fluorescent substrate and specific ACE inhibitor, ramipril (7.81 $\pm$ 1.16 pmol/ml/min). Approximately 132 $\pm$ 19.6 pg of ACE/ml was present in urine. The low level of ACE was also confirmed using ACE-specific substrate hippuryl-L-histidyl-L-leucine, a standard assay described for determining ACE activity (28) (261 $\pm$ 31.1 pg of ACE/ml). By Western analysis a soluble form of ACE2, migrating as a doublet of 105 and 100 KDa, was detected in urine using a polyclonal antibody directed to the 740-amino acid ectodomain of ACE2 (data not shown).

## DISCUSSION

For nearly 60 years, ACE has been considered the central enzyme in the RAS, converting Ang I to the potent vasoconstrictor, Ang II. However, the discovery of other novel RAS components such as the carboxypeptidase ACE2, a homologue of ACE, capable of degrading Ang II and forming Ang (1–7), has emphasized the increasing complexity and multiplicity of biochemical pathways forming the RAS. The present study was prompted by the observation that, although ACE2 and ACE are similar in sequence (~42% identity and ~61% similarity) and are both Type I integral membrane proteins, the two enzymes have quite distinct modes of actions and tissue distribution. This is the first study to characterize ACE2 at the plasma membrane of non-polarized CHO cells and polarized epithelial cells and to compare its cellular localization to its related enzyme, ACE.

At the tissue level, the distribution of ACE2 expression appears to be limited in comparison to the more ubiquitous ACE. Northern blot analysis and real-time PCR studies have shown *ACE2* gene expression to be highest in heart, kidney, testes, and the gastrointestinal tract (2, 3, 18). In the present study, initial attempts were made to identify a human cell line that constitutively expressed ACE2 for cell biology studies. Cell lines originating from renal, cardiac, vascular, and gastrointestinal tissue and transformed and primary cell cultures were screened for ACE2. A transcript encoding ACE2 was detected in all cell lines screened, albeit faintly for ACHN and HEK cells. Overall, the level of activity detected for the translated protein was very low using an ACE2 quenched fluorescent substrate assay and not detectable using immunoblotting or immunofluorescence methodology. Comparatively, the level of activity detected for ACE was 15- to 50-fold greater than that of ACE2. The endogenous expression of ACE in HUVECs, Eahy.926, HCAEC, CF, SVSMC, RPTECs, and CACO-2 is consistent with previous reports (29–31). However, no obvious correlation was observed between the presence of transcript and level of ACE2 catalytic activity, particularly for the transformed cell lines HEK, ACHN, Eahy926, CACO-2, and HT-29. As yet it is not known if post-transcriptional regulation processes such as mRNA stability, translational initiation, and protein stability control the expression of the *ACE2* gene. Such factors may explain the discrepancy observed between mRNA and protein catalytic activity levels observed for ACE2 in the human cell lines screened.

To allow direct biochemical and cellular analysis, recombinant ACE2 and ACE were expressed in CHO cells and MDCKII cells. In both cell types, ACE2 like ACE was observed at the cell surface using the complementary techniques of cell-surface biotinylation and indirect immunofluorescence. However, unlike ACE, which is expressed almost equally at the apical (~55%) and basolateral (~45%) membranes of polarized MDCKII cells, ACE2 is present predominantly at the apical surface (~92%). Several recent studies have localized ACE2 to proximal tubules of human (32), rat (33, 34), and mouse (11) kidney using immunohistochemistry. However, conflict exists as to the exact localization pattern for ACE2 in proximal tubule cells. Some have reported cell surface brush border (apical) staining (11), others cytoplasmic staining (33, 34) or both (abundant brush border and weak cytoplasmic staining) (32). This study presented here has shown unequivocally ACE2 is a cell surface protein and is localized at the apical brush border of proximal tubule cells.

Several mechanisms involved in establishing and maintaining a polarized distribution of membrane proteins in epithelial cells have been documented (35, for review). In MDCK cells, newly synthesized proteins are sorted directly from the *trans*-Golgi network and delivered by transport vesicles to their correct membrane domain (36). Sequence motifs in the cytoplasmic tail of proteins, many of which are related but not identical to endocytic motifs, can confer basolateral sorting (35). Apical sorting signals on the other hand are less well understood and have been identified in the extracellular, transmembrane, and cytosolic regions of proteins (37, 38, 39) and can be encoded by proteinaceous, carbohydrate, and lipid functional groups. The most well described moieties identified with apical sorting are a glycosylphosphatidylinositol (GPI) anchor that associates with lipid raft microdomains (40), and structural post-translational modifications such as *N*-glycosylation (41).

Data from this study suggest that ACE2 and ACE under steady-state conditions occur independent of lipid rafts in non-polarized cells. Neither ACE2 nor ACE possesses a GPI anchor or, as shown in this study, exists in caveolin-rich lipid raft regions of the CHO cell plasma membrane. This observation is consistent with the findings of Parkin *et al.* (20), who also demonstrated that, only in the presence of a GPI anchor, does ACE redistribute from non-raft to raft compartments of the plasma membrane. Nevertheless, further study is required to determine if the pathway taken by ACE2 and ACE is in association with GPI-anchored proteins, which, together with glycosphingolipids, are primarily targeted to the apical domain of MDCK cells (40). Alternatively, *N*-linked glycans may have a role in targeting ACE2 and ACE to the apical surface, because both ACE2 and ACE are extensively *N*-glycosylated proteins, with ~30 and ~40% of their total masses, respectively, being attributed to carbohydrate modification. For human testicular ACE, two of the seven possible glycosylation sites are crucial for correct intracellular transport and cell surface localization (42). No studies have, as yet, described the glycosylation requirements of ACE2.

The possibility that internalization may influence the steady-state distribution of ACE2 and ACE at the cell surface was also investigated in this study. Given that ACE2 is a functional receptor to the SARS coronavirus, as well as its potential role in modulating Ang II actions, understanding the mechanisms that determine the fate of ACE2 at the cell surface is of clear significance. Less than 24% of ACE2 and 13% of ACE internalized from the cell surface after 3 h. Comparison with another type I integral membrane protein, β-amyloid cleaving enzyme-1 (β-secretase or BACE-1), which completely internalizes from the cell surface after 30 min (43), suggests both ACE2 and ACE are inefficiently retrieved from the plasma membrane. The process of internalization is thus a minor contributor to the regulation of ACE2 and ACE at the cell surface. Internalization of ACE is linked to casein kinase-2 phosphorylation and regulates its retention in the endothelial cell plasma membrane of ACE (44). *In vitro* and *in vivo*, ACE is proteolytically cleaved from membrane by the metalloprotease(s) to release a soluble form (45). As we have shown in this study and previously (46), a similar secretion event is observed *in vitro* for ACE2, and can be blocked using a broad-spectrum metalloprotease (sheddase) inhibitor, Ilomastat (47). Here, Ilomastat but not TAPI-2, significantly inhibited the secretion of ACE2 in MDCKII cells. TAPI-2 inhibits ACE secretion ($I_{50}$ of 18 μM (45)). These findings suggest that one or more other sheddases distinct from those involved in ACE secretion may be involved in ACE2 secretion in MDCKII cells. The polarized secretion patterns displayed by ACE2 in MDCKII correlate well with the observation that ACE2 is predominantly apical. Comparatively, ACE is delivered almost equally to both surfaces, but its secretion is 2.5-fold greater at the apical surface than at the basolateral surface. This preferential secretion of ACE may be a novel mechanism for maintaining the distribution of ACE at the cell surface, as well as being a means of regulating the level of soluble ACE. Dempsey and co-workers (48) have also demonstrated differential sheddase activity at the apical and basolateral surfaces of MDCK cells. Preferential secretion of human epidermal growth factor precursor from the basolateral surface in MDCK cells serves to maintain a polarized distribution of epidermal growth factor precursor at the apical surface (48).

The differences in the cell-surface distribution of ACE2 and ACE in MDCKII cells poses the question of their physiological relevance. Both enzymes have been localized by immunohistochemistry to polarized cell types in the kidney; the epithelia of proximal tubules and the endothelia of intrarenal vessels (3, 30, 49, 50). The apical and basolateral distribution of ACE in MDCKII cells is in agreement with studies in humans (51, 52). In human kidney proximal tubular cells, ultrastructural and immunohistochemical localization of ACE is to both the basolateral surface, where ACE contributes to regulation of Ang II-dependent absorption processes and interfaces with the peritubular interstitium (29, 51, 52), as well as to the apical brush borders. Both ACE and neprilysin are prominent enzymes of human kidney brush borders where they metabolize bioactive peptides present in urine following glomerular filtration (52). In this study, we demonstrated the activities of both ACE2 and ACE in human urine, supporting our finding that ACE2, like ACE, is present on the apical surface of renal epithelium and is secreted *in vivo* in humans. Interestingly, the level of soluble ACE2 activity present in human urine was ~10-times greater than the activity observed for ACE. Previous studies have detected ACE in human urine (53). One possibility is that ACE2 has a similar role at the apical surface of renal tubules, participating in an intra-renal RAS by metabolizing Ang II to produce Ang (1–7). Our group has shown that ACE2 has over 12-fold greater catalytic efficiency in degrading Ang II to Ang (1–7) than ACE in producing Ang II from Ang I (54). AT1 receptors, effectors for the physiological actions of Ang II are present in the proximal tubules (55). ACE2 may be an important factor in modulating Ang II at AT1 receptors in normal and disease states. During pregnancy, ACE2 is upregulated in renal tubules found in the cortex and medulla of rat kidney in association with enhanced local production of Ang (1–7) (33). Furthermore, inhibition of ACE and neprilysin using the vasopeptidase inhibitor, omapatrilat, results in an increase of renal ACE2 (mRNA and protein) and Ang (1–7) levels in spontaneously hypertensive rats (56). Treatment of hypertensive patients with omapatrilat also increases the 24-h urinary excretion rates of Ang (1–7) (57). Recently, ACE2 has been identified as a functional receptor for the SARS coronavirus necessary for cell fusion and viral replication (15). This finding also highlights the physiological relevance of ACE2 at the apical surface of epithelial cells this being a potential first site of entry for viral particles and the process of ACE2 solubilization. In conclusion, this study has yielded new insights into the cell-surface localization and the possible mechanisms regulating the steady-state distribution of ACE2 and ACE, and thus a unique insight into the possible physiological roles and regulation of this recently discovered peptidase.

*Acknowledgment—We thank Dr. G. Howell for advice on the bioimaging procedure.*

**REFERENCES**

1. Acharya, K. R., Sturrock, E. D., Riordan, J. F., and Ehlers, M. R. (2003) *Nat. Rev. Drug Discov.* **2,** 891–902
2. Tipnis, S. R., Hooper, N. M., Hyde, R., Karran, E., Christie, G., and Turner, A. J. (2000) *J. Biol. Chem.* **275,** 33238–33243
3. Donoghue, M., Hsieh, F., Baronas, E., Godbout, K., Gosselin, M., Stagliano, N., Donovan, M., Woolf, B., Robison, K., Jeyaseelan, R., Breitbart, R. E., and Acton, S. (2000) *Circ. Res.* **87,** E1–E9
4. Vickers, C., Hales, P., Kaushik, V., Dick, L., Gavin, J., Tang, J., Godbout, K., Parsons, T., Baronas, E., Hsieh, F., Acton, S., Patane, M., Nichols, A., and Tummino P. (2002) *Circ. Res. J. Biol. Chem.* **277,** 14838–14843
5. Guy, J. L., Jackson, R. M., Acharya, K. R., Sturrock, E. D., Hooper, N. M., and Turner, A. J. (2003) *Biochemistry* **42,** 13185–13192
6. Skidgel, R. A. (1985) *Prog. Clin. Biol. Res.* **192,** 371–378
7. Santos, R. A. S., Campagnole-Santos, M. J., and Andrade, S. P. (2000) *Regul. Pep.* **91,** 45–62
8. Zisman, L. S., Keller, R. S., Weaver, B., Lin, Q., Speth, R., Bristow, M. R., and Canver, C. C. (2003) *Circulation* **108,** 1707–1712
9. Zisman, L. S., Meixell, G. E., Bristow, M. R., and Canver, C. C. (2003) *Circulation* **108,** 1679–1681
10. Crackower, M. A., Sarao, R., Oudit, G. Y., Yagil, C., Kozieradzki, I., Scanga, S. E., Oliveira-dos-Santos, A. J., da Costa, J., Zhang, L., Pei, Y., Scholey, J., Ferrario, C. M., Manoukian, A. S., Chappell, M. C., Backx, P. H., Yagil, Y., and Penninger, J. M. (2002) *Nature* **417,** 822–828

11. Tikellis, C., Johnston, C. I., Forbes, J. M., Burns, W. C., Burrell, L. M., Risvanis, J., and Cooper, M. E. (2003) *Hypertension* **41,** 392–397
12. Ye, M., Wysocki J., Naaz, P., Salabat M. R., LaPointe, M. S., and Batlle, D. (2004) *Hypertension* **43,** 1120–1125
13. Donoghue, M., Wakimoto, H., Maguire, C. T., Acton, S., Hales, P., Stagliano, N., Fairchild-Huntress, V., Xu, J., Lorenz, J. N., Kadambi, V., Berul, C. I., and Breitbart, R. E. (2003) *J. Mol. Cell. Cardiol.* **35,** 1043–1053
14. Ishiyama, Y., Gallagher P. E., Averill, D. B. Tallant, A., Brosnihan, K. B., and Ferrario C. M. (2004) *Hypertension* **43,** 970–976
15. Li, W., Moore, M. J., Vasilieva, N., Sui, J., Wong, S. K., Berne, M. A., Somasundaran, M., Sullivan, J. L., Luzuriaga, K., Greenough, T. C., Choe, H., and Farzan, M. (2003) *Nature* **426,** 450–454
16. Kuba, K., Imai, Y., Rao, S., Gao, H., Guo, F., Guan, B., Huan, Y., Yang, P., Zhang, Y., Deng, W., Bao, L., Zhang, B., Liu, G., Wang, Z., Chappell, M., Liu, Y., Zheng, D., Leibbrandt, A., Wada, T., Slutsky, A.S., Liu, D., Qin, C., Jiang, C., and Penninger, J. M. (2005) *Nat. Med.* **11,** 875–879
17. Imai, Y., Kuba, K., Rao, S., Huan, Y., Guo, F., Guan, B., Yang, P., Sarao, R., Wada, T., Leong-Poi, H., Crackower, M. A., Fukamizu, A., Hui, C. C., Hein, L., Uhlig, S., Slutsky, A. S., Jiang, C., and Penninger, J. M. (2005) *Nature* **436,** 112–116
18. Harmer, D., Gilbert, M., Borman, R., and Clark, K. L. (2002) *FEBS Lett.* **532,** 107–110
19. Dales, N. A., Gould, A. E., Brown, J. A., Calderwood, E. F., Guan, B., Minor C. A., Gavin, J. M., Hales, P., Kaushik, V. K., Stewart, M., Tummino, P. J., Vickers, C. S., Ocain, T. D., and Patane, M. A. (2002) *J. Am. Chem. Soc.* **124,** 11852–11853
20. Parkin, E. T., Tan, F., Skidgel, R. A., Turner, A. J., and Hooper, N. M. (2003) *J. Cell Sci.* **116,** 3079–3087
21. Lanctôt, C., Fournier, H., Howell, S., Boileau, G., and Crine, P. (1995) *Biochem. J.* **305,** 165–171
22. Barnes, K., Brown, C., and Turner, A. J. (1998) *Hypertension* **31,** 3–9
23. Gembardt, F., Sterner-Kock, A., Imboden, H., Spalteholz, M., Reibitz, F., Schultheiss, H.-P., Siems, W.-E., and Walther, T. (2005) *Peptides* **26,** 1270–1277
24. Barnes, K., Bourne, A., Cook, P. A., Turner, A. J., and Kenny, A. J. (1991) *Neuroscience* **44,** 245–261
25. Hooper, N. M. (1999) *Mol. Membr. Biol.* **16,** 145–156
26. Ojakian, G. K., and Schwimmer, R. (1988) *J. Cell Biol.* **107,** 2377–2387
27. Gottardi, C. J., and Caplan, M. J. (1993) *Science* **260,** 552–554
28. Barton, M., Carmona, R., Morawietz, H., d'Uscio, L. V., Goettsch, W., Hillen, H., Haudenschild, C. C., Krieger, J. E., Münter, K., Lattmann, T., Lüscher, T. F., and Shaw, S. (2000) *Hypertension* **35,** 329–336
29. Alhenc-Gelas, F., Baussant, T., Hubert, C., Soubrier, F., and Corvol, P. (1989) *J. Hypertens.* (*Suppl.*) **7,** S9–S13
30. Howell, S., Brewis, I. A., Hooper, N. M., Kenny, A. J., and Turner, A. J. (1993) *FEBS Lett.* **317,** 109–112
31. Li, D., Singh, R. M., Liu, L., Chen, H., Singh, B. M., Kazzaz, N., and Mehta, J. L. (2003) *Cardiovasc. Res.* **57,** 238–243
32. Hamming, I., Timens, W., Bulthuis, M. L. C., Lely, A. T., Navis, G. J., and van Goor, H. (2004) *J. Pathol.* **203,** 631–637
33. Brosnihan, K. B., Neves, L. A. A., Joyner, J., Averill, D. B., Chappell, M. C., Sarao, R., Penninger, J., and Ferarrio, C. M. (2003) *Hypertension* **42,** 749–753
34. Li, N., Zimpelmann, J., Cheng, K., Wilkins, J. A., and Burns, K. D. (2005) *Am. J. Physiol.* **288,** 353–362
35. Yeaman, C., Grindstaff, K. K., and Nelson, W. J. (1999) *Physiol. Rev.* **79,** 73–98
36. Wollner, D., and Nelson, W. (1992) *J. Cell Sci.* **102,** 185–190
37. Marzolo, M. P., Bull, P., and Gonzalez, A. (1997) *Proc. Natl. Acad. Sci. U. S. A.* **94,** 1834–1839
38. Dunbar, L. A., Aronson, P., and Caplan, M. J. (2000) *J. Cell Biol.* **148,** 769–778
39. Takeda, T., Yamazaki, H., and Gist Farquhar, M. (2003) *Am. J. Physiol.* **284,** C1105–C1113
40. Brown, D. A., and Rose, J. K. (1992) *Cell* **68,** 533–544
41. Rodriguez-Boulan, E., and Gonzalez, A. (1999) *Trends Cell Biol.* **9,** 291–294
42. Sadhukhan, R., and Sen, I. (1996) *J. Biol. Chem.* **271,** 6429–6434
43. Fluhrer, R., Capell, A., Westmeyer, G., Willem, M., Hartung, B., Condron, M. M., Teplow, D. B., Haass, C., and Walter, J. (2002) *J. Neurochem.* **81,** 1011–1020
44. Kohlstedt, K., Shoghi, F., Müller-Esterl, W., Busse, R., and Fleming, I. (2002) *Circ. Res.* **91,** 749–756
45. Parvathy, S., Oppong, S. Y., Karran, E. H., Buckle, D. R., Turner, A. J., and Hooper, N. M. (1997) *Biochem. J.* **327,** 37–43
46. Lambert, D. W., Yarski, M., Warner, F. J., Thornhill, P., Parkin, E. T., Smith, A. I., Hooper, N. M., and Turner, A. J. (2005) *J. Biol. Chem.* **280,** 30113–30119
47. Levy, D. E., Lapierre, F., Liang, W., Ye, W., Lange, C. W., Li, X., Grobelny, D., Casabonne, M., Tyrrell, D., Holme, K., Nadzan, A., and Galardy, R. E. (1998) *J. Med. Chem.* **41,** 199–223
48. Dempsey, P. J., Meise, K. S., Yoshitake, Y., Nishikawa, K., and Coffey, R. J. (1997) *J. Cell Biol.* **138,** 747–758
49. Defendini, R., Zimmerman, E. A., Weare, J. A., Alhenc-Gelas, F., and Erdös, E. G. (1983) *Neuroendocrinology* **37,** 32–40
50. Danilov, S. M., Faerman, A. I., Printseva, O. Y., Martynov, M. Y., Sakharov, I. Yu., and Trakht, I. N. (1987) *Histochemistry* **87,** 487–490
51. Bruneval, P., Hinglais, N., Alhenc-Gelas, F., Tricottet, V., Corvol, P., Camilleri, J. P., and Bariety J. (1986) *Histochemistry* **85,** 73–80
52. Schulz, W. W., Hagler, H. K., Buja, L. M., and Erdös, E. G. (1988) *Lab. Invest.* **59,** 789–797
53. Kokubu T., and Takada Y. (1987) *Clin. Exp. Hyperten.* [*A*] **9,** 481–485
54. Rice, G. I., Thomas, D. A., Grant, P. J., Turner, A. J., and Hooper N. M. (2004) *Biochem. J.* **383,** 45–51
55. Allen, A. M., Zhuo, J., and Mendelsohn, F. A. O. (2000) *Am. J. Hypertens.* **13,** 31S–38S
56. Flavia F. J., Gupta, M., Gallagher, P. E., Averill, D. A., Crackower, M. A., Penninger, M., Ferrario, C. M., and Chappell, M. C. (2002) *Am. J. Nephrol.* (*Suppl.*) **13,** 146A
57. Ferrario, C. M., Smith, R. D., Brosnihan, B., Chappell, M. C., Campese, V. M., Vesterqvist, O., Liao, W., Ruddy, M. C., and Grim, G. E. (2002) *Am. J. Hypertens.* **15,** 557–564
58. Douglas, G. C., O'Bryan, M. K., Hedger, M. P., Lee, D. K. L., Yarski, M. A., Smith, A. I., and Lew, R. A. (2004) *Endocrinology* **145,** 4703–4711